Korean J. Chem. Eng., 38(1), 64-71 (2021)
DOI: 10.1007/s11814-020-0676-1

pISSN: 0256-1115
eISSN: 1975-7220

Phenol removal via activated carbon from co-pyrolysis of waste coal tar pitch and vinasse

Ming Gao*, Xiaona Wang*, Changlei Xia, Na Song***, Yuhui Ma****, Qunhui Wang*, Tianxue Yang*****, Shengbo Ge**, Chuanfu Wu*,†, and Su Shiung Lam**,******,†**

*Department of Environmental Science and Engineering, School of Energy and Environmental Engineering, University of Science and Technology Beijing, Beijing 100083, China
**Co-Innovation Center of Efficient Processing and Utilization of Forestry Resources, College of Materials Science and Engineering, Nanjing Forestry University, Nanjing, Jiangsu 210037, China
***Department of Environmental Engineering, Tianjin College, University of Science and Technology Beijing, Tianjin 301830, China
****Institute of Seawater Desalination and Multipurpose Utilization, Ministry of Natural Resources, Tianjin 300192, China
*****State Key Laboratory of Environmental Criteria and Risk Assessment, Chinese Research Academy of Environmental Sciences, Beijing 100012, China
******Institute of Tropical Aquaculture and Fisheries (AKUATROP), Universiti Malaysia Terengganu, 21030 Kuala Terengganu, Terengganu, Malaysia
(*Received 18 July 2020 • Revised 2 September 2020 • Accepted 10 September 2020*)

Abstract−The behavior and characteristics of phenol adsorption by activated carbon produced from co-pyrolysis of coal tar pitch and vinasse were investigated. Coal tar pitch and vinasse (mass ratio of 1 : 3) were firstly co-pyrolyzed and carbonated at 400 °C for 2 h. The carbonized material produced was then soaked with saturated KOH solution and activated at 800 °C for 1 h to form activated carbon. Results from the phenol wastewater adsorption experiments suggest that pseudo-second-order kinetics and the Weber-Morris model could reflect the time-dependent adsorption behavior of phenol wastewater by the activated carbon, revealing that internal diffusion represents the rate-limiting procedure and dominant process to control the adsorption rate in the early stage of the adsorption. Monolayer adsorption played the key role during the phenol adsorption. The adsorption was an endothermic reaction in temperature ranging from 15 °C to 35 °C, indicating that the adsorption speed could be stimulated by the increasing temperature. This study establishes a theoretical foundation for the usage and the potential application of the activated carbon derived from coal tar pitch and vinasse in wastewater treatment.

Keywords: Coal Tar Pitch, Vinasse, Activated Carbon, Phenol Wastewater, Adsorption Kinetics and Thermodynamics

INTRODUCTION

Activated carbons can be extensively used in diverse industries, for instance, food [1], chemical [2], electric power [3], environmental protection [4-7], gas separation and storage [8]. The typical raw materials of activated carbons are mainly biomass and minerals, for example, shells, bamboo [9-11] and coal [12]. Because of limited natural resources, the use of the typical raw materials to prepare activated carbons was restricted in these years [13]. Therefore, finding some substitute carbonaceous wastes (e.g., household garbage, sewage sludge, waste tires, waste plastics) for activated carbon preparation is critical and has become a research hotspot [14-16].

Coal tar pitch (abbreviated to CTP hereafter), a waste residue generated during coal tar distillation, was mainly used in the manufacture of electrolytic aluminum anode in China in the past few years. However, increasing generation of CTP, especially the medium-temperature-produced CTP, has been stocked these days due to the recession of the aluminum electrolysis industry [17]. It is important to find an alternative and efficient way for the recycling of CTP [18,19]. Given the high elemental carbon content, medium-temperature-produced CTP shows to be transformed into activated carbon. However, the presence of light chemical components might volatize during the pyrolysis of CTP, leading to potentially low production the solid pyrolysis products (i.e., activated carbon).

Vinasse, a typical representative of cellulosic waste, contains a large fraction of crude fiber [20,21], owing to this property, the preparation of activated carbons by vinasse has emerged [22,23]. These studies strongly demonstrated that vinasse is particularly suitable for pyrolysis into activated carbon owing to its satisfactory thermosetting performance. This provides the motivation for co-pyrolyzing CTP and vinasse followed by activation to produce activated carbon with potentially desirable properties.

In China, the CTP generation was about 6.684 million in 2019 (Data from the China Coking Industry Association, CCIA 2020), while the vinasse also had a high annual production of approximately 100 million tons [24]. Preparation of activated carbons using

†To whom correspondence should be addressed.
E-mail: wucf@ustb.edu.cn, lam@umt.edu.my

the mixture of the CTP and vinasse might be a sensible solution for dealing with the disposal of CTP. Consequently, in this study, the production and characteristics of activated carbon prepared from co-pyrolysis of CTP and vinasse as raw materials were investigated. The optimal operational parameters, including the initial pH, adsorption time and temperature, were determined. In addition, the adsorption behavior of phenol by activated carbon was also explored. The adsorption kinetics and modelling are analyzed and discussed. This study might establish a theoretical foundation for the usage and the potential application value of the co-pyrolysis of CTP and vinasse in wastewater treatment.

EXPERIMENTAL

1. Materials

Medium-temperature-produced CTP was obtained from a coking plant located in Hebei, China, and the vinasse was collected from a spirit distillery in Beijing, China. The main properties of medium-temperature-produced CTP and vinasse are shown in Table 1 and Table 2, respectively. Before the experiment, the leaching toxicity of coal pitch was examined. Inductively coupled plasma mass spectrometry (ICP-MS) (Agilent 7700; Agilent Technologies, Palo Alto, CA, USA) was implemented to determine the concentration of Pb, Cu, Cd, Ni, Zn, and Cr in the leaching agent. In the leaching solution, the Cu ion concentration was 36 $\mu g \cdot L^{-1}$ which was lower than the limitation of 1.0 $mg \cdot L^{-1}$ documented in Chinese Standard GB 5749-2006. On the other hand, the concentration of the rest of the heavy metal was all below the detection limitation of ICP and apparently met the requirement of GB 5749-2006.

2. Activated Carbon Preparation

2-1. Co-pyrolysis and Carbonization Process

CTP and vinasse were mixed at a mass ratio of 1 : 3 and dissolved in dichloromethane (mixture medium). The mixture was stirred evenly and then allowed to dry in air for subsequent application. Afterward, the mixture was placed in a high-temperature tube furnace (OTF-120-X-S, manufactured by Hefei Kejing Company Limited) for carbonization. Nitrogen was used as the shielding gas in the pyrolysis process. The resistance furnace was heated to 400 °C at a rate of 5 °C·min^{-1} and then maintained for 2 h. The carbonized materials obtained by pyrolysis were crushed and sieved to 20-40, 40-80 and 80-100 mesh before further use.

Table 1. Chemical composition of the medium temperature coal tar pitch (%)

BI[a]	QI[b]	C	H	S	O
30.5	4.3	90.5	4.1	0.8	3.2

[a]BI stands for the toluene insoluble material
[b]QI stands for the quinolone insoluble material

Table 2. Chemical composition of the vinasse (dry basis, %)

Cellulose	Lignin	Hemi-cellulose	Protein	Starch	Fat	Ash
41.3	25.4	20.6	7.7	3.1	1.4	0.5

2-2. Activation Process

Ground carbonized material was impregnated with KOH solution (42.9 wt%) using the carbon/KOH weight ratio of 1 : 1, 1 : 2, 1 : 3, 1 : 4, respectively (hereinafter referred to as the impregnation ratio), and the impregnation time was 0 min, 30 min and 60 min. The immersed materials were dried and then placed in the high-temperature tube furnace for activation with nitrogen as the shielding gas. The resistance furnace was heated to 800 °C at a rate of 10 °C·min^{-1} and then remained for 30 min, 60 min, 90 min, respectively. The activated carbon product was washed with distilled water after activation to wash away the activated material until the flushing solution was neutral. Then, suction filtration was conducted, and dried under 105 °C, after which the activated carbon product was obtained.

3. Determination of Iodine Adsorption Value

The iodine sorption value and liquid-phase adsorption properties (e.g., methylene blue decolorization capacity and caramel decolorization capacity) are the common indexes representing the adsorption ability of activated carbon and serve as some critical indexes for evaluating the industrial activated carbon in Chinese enterprises. These indexes have great practical value. Therefore, the iodine sorption value was also determined in this study to evaluate the adsorptive property. The iodine sorption values were measured based on GB/T 7702.7-2008.

4. Adsorption of Phenol Wastewater

A total of 0.025 g activated carbon product and 30 mL phenol solution of a certain concentration was added to a conical flask. The pH value was adjusted by HCl and NaOH with 0.1 $mol \cdot L^{-1}$. The mouth of the flask was then sealed. The flask was placed in a constant-temperature vibrator for vibration and adsorption at a rate of 150 $r \cdot min^{-1}$ for a certain amount of time. A certain amount of solution obtained passed through a 0.45 μm filter membrane. The absorbance was determined by an ultraviolet spectrophotometer with maximum adsorption wavelength (270 nm) of phenol. The concentration was calculated with the standard curve.

4-1. Adsorption Kinetics Experiment

A 30 mL phenol solution was added to several conical flasks with capacity of 50 $mg \cdot L^{-1}$. After adjusting the solution to an appropriate pH value, these conical flasks were placed in a vibrator at a rate of 150 $r \cdot min^{-1}$ and temperature of 25 °C to conduct experiments for different adsorption times. Certain solutions were obtained to be filtered with a filter membrane. The absorbance values were measured, and the concentrations were calculated by a standard curve. Pseudo-first-order (Eq. (1)) and pseudo-second order (Eq. (2)) kinetics models were used to fit the course of activated carbon adsorption of phenolic wastewater.

$$q_t = q_e[1 - \exp[-(k_1 t)]] \quad (1)$$

$$q_t = \frac{k_2 q_e^2 t}{1 + k_2 q_e t} \quad (2)$$

where k_1 (min^{-1}) and k_2 ($g \cdot mg^{-1} \cdot min^{-1}$) are the adsorption rate constants of the pseudo-first-order equation and pseudo-second-order equation, respectively; q_t ($mg \cdot g^{-1}$) and q_e ($mg \cdot g^{-1}$) are the adsorption capacity at time t (min) and under equilibrium state, respectively.

Linear representation of pseudo-first-order (Eq. (3)), pseudo-

second-order (Eq. (4)) models is as follows:

$$\log(q_e - q_t) = \log q_e - \frac{k_t t}{2.303} \quad (3)$$

$$\frac{t}{q_t} = \frac{t}{q_e} + \frac{1}{k_2 q_e^2} \quad (4)$$

Besides, the adsorption process is affected by the interaction between the absorbed substance and adsorbent and is related to the diffusion mechanism of the absorbed substance in the holes of the adsorbent. The Weber-Morris model could be adopted to study the diffusion mechanism of absorbed substance [25,26]. The definition of the model is as follows (Eq. (5)).

$$q_e = k_i t^{0.5} + C_i \quad (5)$$

where k_i ($mg \cdot g^{-1} \cdot min^{-0.5}$) is in-particle diffusion rate constant; C_i ($mg \cdot g^{-1}$) is the intercept, reflecting the thickness of the boundary layer. And the larger the C_i value is, the larger the boundary layer effect is. If q_e–$t^{0.5}$ is a straight line and passes the origin, the rate controlling procedure only depends on in-particle internal diffusion.

4-2. Adsorption Thermodynamics Experiment

A total of 30 mL phenol solutions with 10, 20, 30, 50, and 70 mgL^{-1} were added to different conical flasks. After adjusting the pH value, the flasks were placed in the constant-temperature vibrator to conduct experiments for a certain time at temperatures of 15, 25, and 35 °C. Certain solutions were obtained to be filtered with a filter membrane. The absorbance values were measured, and the concentration of the phenol solutions was calculated by a standard curve. Langmuir (Eq. (6)) and Freundlich (Eq. (7)) models can be applied to fit the adsorption isotherms.

$$q_e = \frac{q_m K_L C_e}{1 + K_L C_e} \quad (6)$$

$$q_e = K_F C_e^{1/n} \quad (7)$$

where q_m ($mg \cdot g^{-1}$) is the maximum monolayer adsorption capacity of activated carbon; K_L ($L \cdot mg^{-1}$) is the Langmuir constant; K_F ($mg \cdot g^{-1}$) ($L \cdot mg^{-1}$)$^{1/n}$ is the Freundlich adsorption constant; 1/n (−) reflects the adsorption intensity; C_e ($mg \cdot g^{-1}$) means the concentration of adsorbate under adsorption equilibrium condition.

Linear forms of the above isotherm models are as follows:

$$\frac{C_e}{q_e} = \frac{1}{q_m} C_e + \frac{1}{K_L q_m} \quad (8)$$

$$\ln q_e = \frac{1}{n} \ln C_e + \ln K_F \quad (9)$$

Thermal changes during the adsorption process cause changes in thermodynamic parameters, including Gibbs free energy (ΔG^0), enthalpy (ΔH^0), and entropy (ΔS^0), which help to make the adsorption mechanism more clear. Thermodynamic calculations for the process of activated carbon absorbing phenolic wastewater were conducted by the variation in the *van't Hoff* equation (Eq. (10)).

$$\ln K_v = -\frac{\Delta H^0}{R}\frac{1}{T} + \frac{\Delta S^0}{R} \quad (10)$$

where K_v ($L \cdot mg^{-1}$) (defined as C_s/C_e) is the van't Hoff constant; C_s ($mg \cdot g^{-1}$) is the concentration reduction of adsorbate induced by the adsorption of the adsorbent under adsorption equilibrium condition; R (8.314 $J \cdot mol^{-1} \cdot K^{-1}$) is the universal gas constant; T (K) is the absolute solution temperature; ΔH^0 ($J \cdot mol^{-1}$) is the enthalpy change; ΔS^0 ($J \cdot K^{-1}$) is the entropy change.

RESULTS AND DISCUSSION

It is generally known that the iodine value of activated carbon is affected by the impregnation ratio of activator to carbon material, impregnation time, activation time and particle size of carbon material. Therefore, according to the experimental method described in section 2.2, the influence of the above factors on the iodine value of activated carbon was investigated by single variable method. The results are shown in Fig. 1.

1. Effect of Impregnation Condition on the Iodine Value of the Activated Carbon

The effects of impregnation ratio and impregnation time on iodine value of activated carbon were investigated under the condition of carbon particle size of 20-40 mesh and activation time of 60 min. As shown in Fig. 1(a), the iodine value of activated carbon increased with the increase of impregnation ratio. These signs indicated that the KOH dynamic allocation process occurred between pyrolytic carbon and impregnating solution during the impregnation period. When the impregnation ratio was low, the

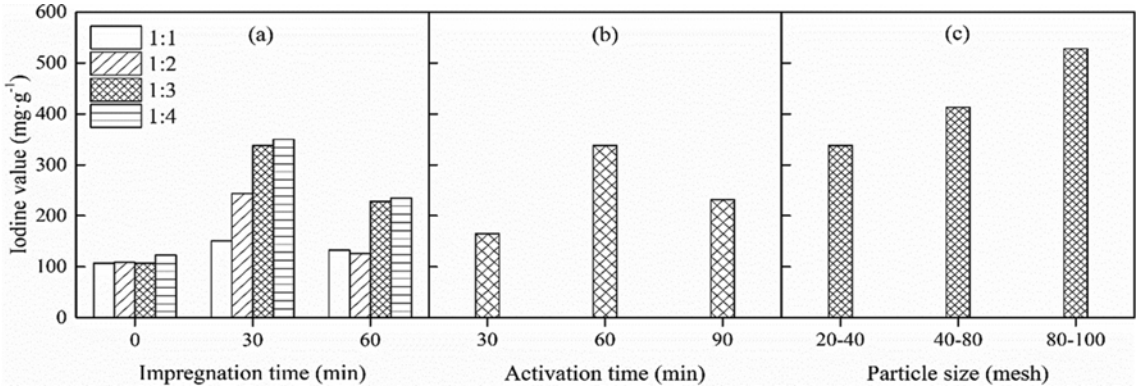

Fig. 1. Iodine value of the activated carbon acquired under different impregnation conditions: (a) Impregnation time, (b) activation time, (c) particle size.

KOH concentration gap between the pyrolytic carbon and impregnating solution was small. Thus, the KOH dynamic allocation rate to the pyrolytic carbon was slow, and much time was consumed for a sufficient amount of activating agent to attach to the pyrolytic carbon. Even if the dynamic allocation process reaches equilibrium, the KOH on the solid phase may still be insufficient. When the impregnation ratio was large, the KOH concentration gap between the pyrolytic carbon and impregnating solution was large. Thus, the KOH dynamic allocation rate to pyrolytic carbon was fast, and only a small amount of time was required for the activating agent to attach to the pyrolytic carbon. However, when the impregnation ratio increased from 1 : 3 to 1 : 4, the iodine value of activated carbon increased by 3.6% at most. Therefore, to maximize the utilization rate of KOH, 1 : 3 was selected as an optimal impregnation ratio of this study. Moreover, Zhu et al. demonstrated that during the impregnation process with a KOH solution, increasing the impregnation time within a certain range causes potassium ion to enter the holes of cellulose, thereby benefiting the creation of activated carbon holes [27]. However, if the impregnation time is too long, the micropores would be corroded to the mesopores, even the macro pores, leading to a decrease in the iodine sorption value. In summary, in our study, the optimum impregnation conditions were identified as impregnation ratio of 3 : 1 and impregnation time of 30 min, which will be used in the following experiments.

2. Effect of the Activation Time on the Iodine Value of the Activated Carbon

In this part, when pyrolytic carbon size was 20-40 mesh, impregnation ratio was 3 : 1, and immersion time was 30 min, three activation times (30, 60, and 90 min) were selected to study the effect on the final product (i.e., the activated carbon). From Fig. 1(b), iodine values of the prepared activated carbons were 165, 338, 232 $mg \cdot g^{-1}$ when the activation time was 30, 60, 90 min, respectively. The shorter activation time (e.g., 30 min) made the activation reaction between KOH and chars insufficient, fewer pores were created, resulting in low iodine value. On the other hand, when the activation time was long (e.g., 90 min), the activation reaction between KOH and pyrolytic carbon was excessive, resulting in the pores collapsing and the micropores transforming into a large hole. As a result, the iodine value of the prepared activated carbons decreased. The optimum activation time in this experiment was 60 min in terms of interspace formation of the pyrolytic carbon. Therefore, activation time of 60 min was adopted in the ensuing experiments.

3. Effect of Particle Sizes on the Iodine Value of the Activated Carbon

The pyrolytic carbons were ground to particle sizes of 20-40, 40-80, and 80-100 mesh. Moreover, it might have caused energy dissipation when the particle size was higher than 100 mesh; thus, this situation was not investigated in the study. The rest of the factors including impregnation ratio, impregnation time and activation time were 3 : 1, 30 min and 60 min. As shown in Fig. 1(c), when particle size of chars was 20-40, 40-80, and 80-100 mesh, the iodine values of the prepared activated carbons were 338, 413, 528 $mg \cdot g^{-1}$, respectively. The highest (528 $mg \cdot g^{-1}$) occurred in particle size of 80-100 mesh. It could be attributed to the following reason: first, when the particle size was large (i.e., 20-40 mesh), the contact area between the activator and the pyrolytic carbon was small and it was difficult for the activator to penetrate into the internal space of the pyrolytic carbon. The amount of KOH in the pyrolytic carbon was insufficient, leading to the insufficient activation. On the other hand, when the particle size was small (i.e., 80-100 mesh), the contact area between the activator and char was large. The activator could smoothly migrate into the internal part of the pyrolytic carbon and the activation reaction could be carried out successfully, increasing the increment of the iodine value of the activated carbons.

In summary, the largest activated carbon iodine value appeared at the following condition: impregnation time of 30 min, particle size within 80-100 mesh, impregnation ratio of 3 : 1 and activation time of 60 min. Therefore, the activated carbon applied in the following study was generated under this optimal condition.

4. Characterization of the Activated Carbon Produced under the Optimum Condition

The specific surface area of activated carbon prepared under the optimal conditions was 1,027 $m^2 \cdot g^{-1}$ (Table 3). It is demonstrated that KOH was a suitable agent for the activation of the pyrolytic carbon synthesized from the mixture of coal tar pitch and vinasse. In addition, the mesopore volume (V_{meso}=0.1 $cm^3 \cdot g^{-1}$) is lower than that of the micropore (V_{micro}=0.4 $cm^3 \cdot g^{-1}$), suggesting that the micropores were the main constituent of this activated carbon.

5. Study of the Mechanism of Phenol Adsorption by the Prepared Activated Carbon

Presently, numerous researches have reported the application of CTP-based activated carbon [28] on wastewater treatment in terms of heavy metal removal [29,30] and organic contaminant adsorption [31,32]. In this study, after determining the iodine values, which reflected the basic adsorption capacities of activated carbon, phenol served as the target material for adsorption experiments to further explore the adsorption capacity on organic pollutants. Furthermore, the effects of phenol solution initial pH value, adsorption time, and adsorption temperature on the adsorption performances were explored.

5-1. Effect of Initial Solution pH Values on the Removal Rate of the Phenol

From Fig. 2, the removal rate of phenol changed with initial phenol solution pH value and the removal rates were low when the pH value was lower than 7. It might be because the degree of phenol dissociation was negligible when the pH value of the solution ranged from neutral (i.e., 6.9) to acidic (i.e., 3.2) and most of

Table 3. Specific surface area and pore volumes of activated carbon produced under the optimum conditions

Sample	S_{BET} (m^2g^{-1})	V_{total} (cm^3g^{-1})	V_{micro} (cm^3g^{-1})	V_{meso} (cm^3g^{-1})	Yield
Activated carbon	1027	0.6	0.4	0.1	30.2%

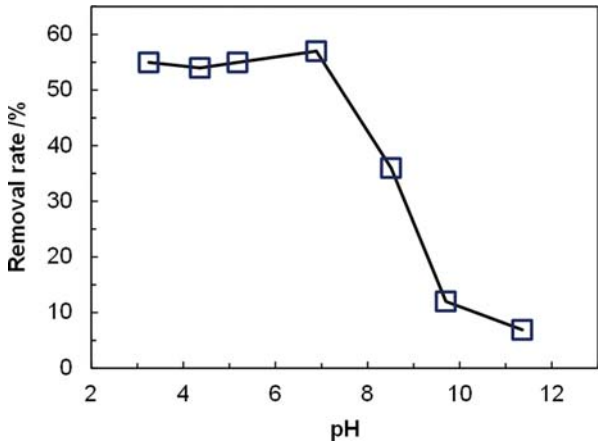

Fig. 2. Relationship between phenol solution's initial pH values and phenol removal rates (Initial concentration of phenol=50 mg·L^{-1}, Activated carbon dosage=0.025 g).

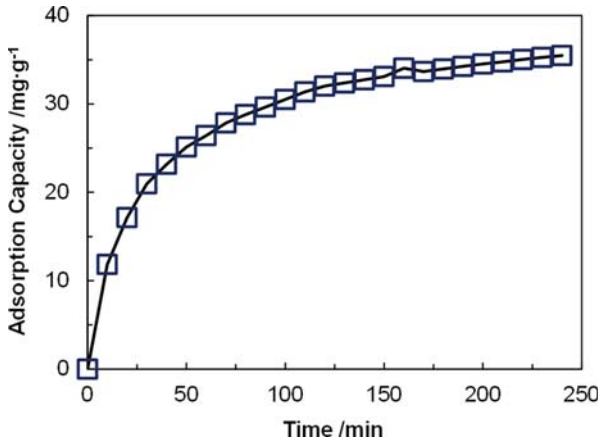

Fig. 3. Effect of adsorption time on adsorption capacity (Initial concentration of phenol=50 mg·L^{-1}, Activated carbon dosage= 0.025 g).

the phenol existed as the molecular state, which facilitated the removal of phenol. On the other hand, when the solution was alkaline, phenol molecules disintegrated into hydrogen ion and oxygen anion benzene (with strong polarity). Given the weak adsorption ability of activated carbon for polar organic matter, it went bad under alkaline conditions. Therefore, the optimal pH value for activated carbon to adsorb was neutral to acidic and the pH in the adsorption environment was adjusted to approximately 6.5 in the following experiments.

5-2. Effect of the Adsorption Time on the Removal Rate of Phenol and Research on Adsorption Dynamics

As displayed in Fig. 3, the removal rate of phenol by activated carbon initially increased and then decreased into equilibrium with the extension of time. The adsorption process was slow, perhaps because of the diffusion processes of molecules inside adsorbent holes. When the adsorption time was 200 min, the adsorption achieved a balance basically, with an adsorption capacity of approximately 36 mg·g^{-1}. In the first 50 min, the adsorption speed was high and the adsorption capacity reached 25 mg·g^{-1} (i.e., 71% of the equilibrium adsorption capacity). After 50 min, the adsorption speed decreased. In the subsequent 2 h, the adsorption capacity merely increased by 10 mg·g^{-1}. Thus the adsorption of phenol by activated carbon reached equilibrium at 200 min.

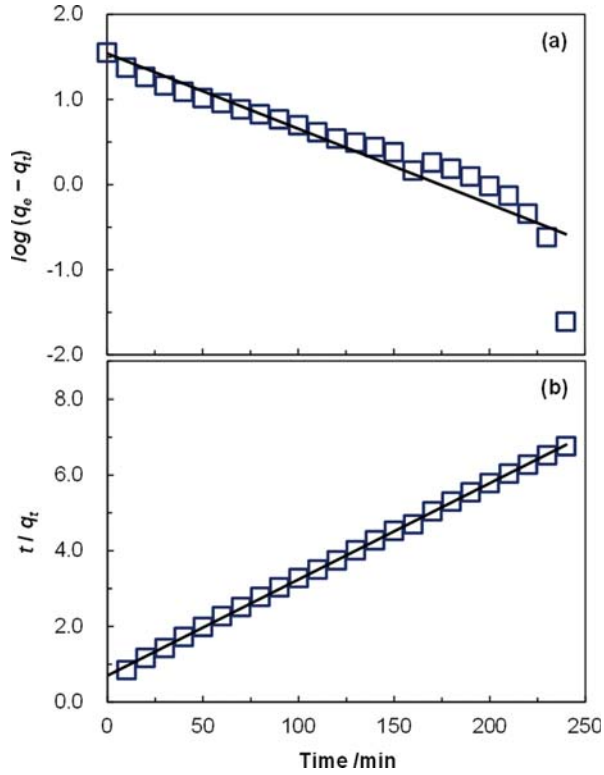

Fig. 4. Model of pseudo-first-order (a) and pseudo-second-order (b) (Initial concentration of phenol=50 mg·L^{-1}, Activated carbon dosage=0.025 g).

The adsorption dynamical behavior of activated carbon performed by the first-order kinetic equations and second-order kinetic equations is displayed in Fig. 4. Given that the R^2 value was close to 1 (from Table 4), the second-order kinetic model could describe the adsorption of phenol wastewater by activated carbon successfully, which revealed the adsorption process might involve the chemical reactions, induced by complicated functional groups.

5-3. Particle Diffusion Model of Weber-Morris

As shown in Fig. 5 and Table 5, linear fitting for the adsorption

Table 4. Parameters of the adsorption kinetics model

Pseudo-first-order			Pseudo-second-order		
k_1 (min^{-1})	q_e (mg·g^{-1})	R^2	k_2 (g·mg^{-1}·min^{-1})	q_e (mg·g^{-1})	R^2
0.020	35.0	0.88	0.0009	39.4	0.9996

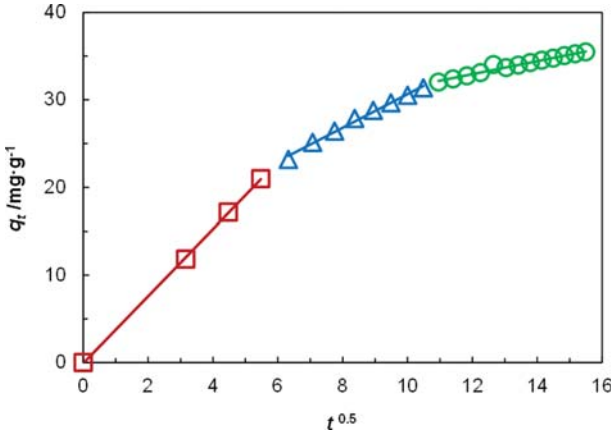

Fig. 5. Fitting line of the model of Weber-Morris (Initial concentration of phenol=50 mg·L^{-1}, Activated carbon dosage=0.025 g).

Table 5. Model parameters of Weber-Morris

Stages	k_i (mg·g^{-1}·min$^{-0.5}$)	C_i	R_i^2
First stage	3.8	−0.07	0.9998
Second stage	1.9	11.4	0.9929
Third stage	0.7	24.0	0.9713

data of phenol was conducted with the model of Weber-Morris. The adsorption fitting line of phenol by activated carbon could be segmented into three stages: a sharp raise, a less step raise and a plateau. In the sharp raise stage (first stage), internal diffusion phenomenon occurred in the mesopores or macropores in terms of the little intercept of the curve and it was the adsorption rate-limiting step. On the other hand, the predominant step of the second stage might be the internal diffusion in the micropores suggestion from the large intercept and correlation coefficient of the curve and the third stage was the adsorption equilibrium phase. In the third stage, the fitting correlation coefficient was relatively small and the intercept was large. It might be because the boundary-layer thickness was enlarged with the adsorption, hindering the mass transfer. In light of the slopes of the three stages, the following conclusions could be drawn: the diffusion force and rate decreased with the adsorption time. It could be attributed to the fact that phenol molecules might narrow and block the activated carbon pore during the adsorption period.

5-4. Effect of Adsorption Temperature on the Removal Rates of Phenol and Research on Adsorption Thermodynamics

Fig. 6 confirms that the Langmuir and Freundlich model could fit the phenol adsorption isotherms of the activated carbon. The

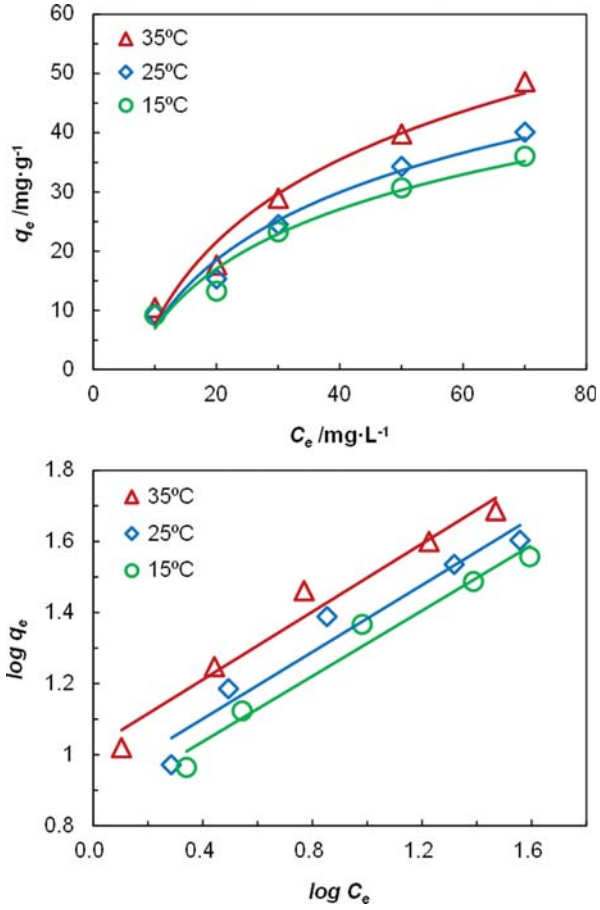

Fig. 6. Fitting line of the Langmuir and Freundlich models (Initial concentration of phenol=10, 20, 30, 50, 70 mg·L^{-1}, Activated carbon dosage=0.025 g).

parameters of the two models are listed in Table 6. Langmuir adsorption principle was more suitable for the description of the phenol in terms of coefficients of determination, indicating that the phenol adsorption by the activated carbon was monolayer adsorption. In addition, the theoretical saturated phenol adsorption capacity increased with temperature. The saturated adsorption reached a maximum value of 57.5 mg·g^{-1} at 35 °C. It indicated that raising temperature of the solution was conducive to phenol adsorption. In the Langmuir model, R_L (R_L=1/(1+K_LC_0) is a dimensionless separation factor; C_0 (mg·g^{-1}) means the original concentration the adsorbed substances) was adopted to indicate the extent of the adsorption [33]. According to the calculation, R_L of this experiment ranged from 0.08 to 0.45, which was within the range of 0 to 1, suggesting that phenol adsorption by the prepared acti-

Table 6. Model parameters

Temperature	Langmuir			Freundlich		
	Q_m (mg·g^{-1})	K_L (L·mg^{-1})	R^2	K_F (mg·g^{-1}) (L·mg^{-1})$^{1/n}$	1/n	R^2
15 °C	42.7	0.12	0.9970	2.8	0.478	0.9715
25 °C	47.6	0.14	0.9978	2.5	0.470	0.9457
35 °C	57.5	0.16	0.9952	2.3	0.461	0.9681

Table 7. Parameters of the adsorption thermodynamics

Concentration ($mg \cdot L^{-1}$)	ΔH^0 ($J \cdot mol^{-1}$)	ΔS^0 ($J \cdot mol^{-1} \cdot K^{-1}$)	ΔG^0 ($KJ \cdot mol^{-1}$)			R^2
			15 °C	25 °C	35 °C	
10	2.6	31.9	−9.2	−9.5	−9.8	0.9069
20	6.7	39.3	−11.3	−11.7	−12.1	0.9995
30	2.8	31.0	−8.9	−9.2	−9.6	0.9850
50	3.0	29.0	−8.3	−8.6	−8.9	0.9953
70	3.2	27.9	−8.0	−8.3	−8.6	0.9497

vated carbon was incidental. The same conclusion could also be obtained from the fitting results of the Freundlich model (i.e., $0.1 < 1/n < 0.5$).

Thermodynamics analysis showed that the Gibbs free energy changes ΔG^0 of the adsorption reaction under the selective temperatures and phenol concentrations were all above 0, as displayed in Table 7, indicating that the adsorption of activated carbon on phenol under various conditions was basically a spontaneous behavior. In addition, ΔG^0 was within range of -20-0 KJ mol^{-1}, which generally revealed that physical adsorption was the predominant process during phenol adsorption. Furthermore, the ΔH^0 and ΔS^0 were all above 0, revealing that the adsorption reaction was endothermic and the degrees of the freedom of the system increased compared with the original status. The result was contrary to the traditional understanding that the adsorption process was an entropy-reduce and exothermic process. A possible explanation to this phenomenon might be because, generally, in a closed system, adsorption might reduce the degrees of the freedom of the system and it was indeed an exothermic process. However, the pH value of the system was adjusted by the HCl solution during the adsorption process (i.e., open system), leading to the increase of the freedom degree of the system. And according the calculation of *van't Hoff* equation (2.10), this operation might change the reaction from exothermic into endothermic. Therefore, rising temperature was beneficial to the stimulation of adsorption rate of the phenol by the prepared activated carbon under the pH adjusted conditions, as evidenced from the reduced values of ΔG^0 with increasing solution temperature.

CONCLUSIONS

Activated carbon was successfully produced from co-pyrolysis of CTP and vinasse combined with KOH activation. The suitable operating conditions were as follows: particle size within range 80-100 mesh, impregnation ratio (mass ratio of KOH and charcoal material) of 3 : 1, soaking period of 30 min, and activation period of 60 min.

The optimal adsorptive property of activated carbon was achieved under this condition, corresponding to an iodine value of 528 $mg \cdot g^{-1}$. The adsorption time required by the prepared activated carbon to reach saturation equilibrium for the adsorption of the phenol was 200 min. The adsorption process highly coincided with the Langmuir isotherms, indicating that monolayer adsorption played a major role. Through calculation, the theoretical maximal absorbing capacity was 57.5 $mg \cdot g^{-1}$. In the temperature range from 15 to 35 °C, the adsorption of phenol solution by activated carbon under pH adjusted condition was an endothermic reaction and high temperatures were beneficial to the phenol adsorption.

ACKNOWLEDGEMENTS

This work was supported by the Guangxi Key Research and Development Program (Guike AB18126087) and the National Key R&D Program (2018YFC1900904). The support from Sino-US-Japan Joint Laboratory on Organic Solid Waste Resource and Energy Technology of USTB is appreciated. Universiti Malaysia Terengganu under Golden Goose Research Grant Scheme (GGRG) (UMT/RMIC/2-2/25 Jld 5 (64), Vot 55191) for supporting Dr. Lam to perform this joint project.

REFERENCES

1. M. Olivares-Marin, V. Del Prete, E. Garcia-Moruno, C. Fernandez-Gonzalez, A. Macias-Garcia and V. Gomez-Serrano, *Food Control*, **20**, 298 (2009).
2. A. Martínez de Yuso, M. Teresa Izquierdo, R. Valenciano and B. Rubio, *Fuel Process. Technol.*, **110**, 1 (2013).
3. R. Yavuz, H. Akyildiz, N. Karatepe and E. Etinkaya, *Fuel Process. Technol.*, **91**, 80 (2010).
4. F. Kaouah, S. Boumaza, T. Berrama, M. Trari and Z. Bendjama, *J. Clean. Prod.*, **54**, 296 (2013).
5. C. Peng, X. Yan, R. Wang, J. Lang, Y. Ou and Q. Xue, *Electrochim. Acta*, **87**, 401 (2013).
6. K. Yaghmaeian, G. Moussavi and A. Alahabadi, *Chem. Eng. J.*, **236**, 538 (2014).
7. Q. Gao, H. Liu, C. Cheng, K. Li, J. Zhang, C. Zhang and Y. Li, *Powder Technol.*, **249**, 234 (2013).
8. A. Yamashita, Y. Mori, T. Oshima and Y. Baba, *Carbon*, **76**, 53 (2014).
9. J. Xu, L. Chen, H. Qu, Y. Jiao, J. Xie and G. Xing, *Appl. Surf. Sci.*, **320**, 674 (2014).
10. S. Yorgun, N. Vural and H. Demiral, *Micropor. Mesopor. Mater.*, **122**, 189 (2009).
11. Y. Wang, H. Ngo and W. Guo, *Sci. Total Environ.*, **533**, 32 (2015).
12. X. Yao, J. Liu, G. Gong, Y. Jiang and Q. Xie, *Int. J. Min. Sci. Tech.*, **23**, 395 (2013).
13. S. Ge, Y. Wu, W. Peng, C. Xia, C. Mei, L. Cai, S. Shi, C. Sonne, S. S. Lam and Y. F. Tsang, *Chem. Eng. J.*, **385**, 123949 (2020).
14. S. Ge, S. Y. Foong, N. L. Ma, R. K. Liew, W. A. Wan Mahari, C. Xia, P. N. Y. Yek, W. Peng, W. L. Nam, X. Y. Lim, C. M. Liew, C. C. Chong, C. Sonne and S. S. Lam, *Renew. Sust. Energ. Rev.*, **127**, 109871

(2020).
15. Y. Wu, C. Xia, L. Cai and S. Q. Shi, *J. Colloid Interface Sci.*, **518**, 41 (2018).
16. C. Xia and S. Q. Shi, *Green Chem.*, **18**, 2063 (2016).
17. H. Chang, W. Wei, Z. Wang, H. Yang and R. Yao, *Shanxi Coking Coal Sci. Tech.*, **2**, 39 (2007).
18. K. S. Yang, D. J. Lee, S. K. Ryu, Y. Korai, Y. J. Kim and I. Mochida, *Korean J. Chem. Eng.*, **16**, 518 (1999).
19. Y. Wu, L. Cai, C. Mei, S. S. Lam, C. Sonne, S. Q. Shi and C. Xia, *Mater. Today Commun.*, **24**, 101008 (2020).
20. M. Ul-Islam, M. W. Ullah, S. Khan and J. K. Park, *Korean J. Chem. Eng.*, **37**, 925 (2020).
21. Y. Wu, S. Ge, C. Xia, L. Cai, C. Mei, C. Sonne, Y. Park, Y. Kim, W. Chen, J. Chang and S. S. Lam, *Bioresour. Technol.*, **313**, 123675 (2020).
22. Y. Ma, R. Niu, X. Wang, Q. Wang, X. Wang and X. Sun, *Waste Manag. Res.*, **32**, 1123 (2014).
23. H. Wang, R. Xie, J. Zhang and J. Zhao, *Adv. Powder Technol.*, **29**, 27 (2018).
24. X. Zhang, H. Tang, G. Chen, L. Qiao, J. Li, B. Liu, Z. Liu, M. Li and X. Liu, *Eur. Food Res. Technol.*, **245**, 2631 (2019).
25. K. Y. Foo and B. H. Hameed, *Bioresour. Technol.*, **112**, 143 (2012).
26. A. K. Prajapati and M. K. Mondal, *Korean J. Chem. Eng.*, **36**, 1900 (2019).
27. Y. Zhu, W. Du, Y. Su and M. Zhu, *Chin. Agr. Sci. Bull.*, **31**, 26 (2015).
28. B. Tsyntsarski, B. Petrova, T. Budinova, N. Petrov, D. K. Teodosiev, A. Sarbu, T. Sandu, M. Ferhat Yardim and A. Sirkecioglu, *Desalin. Water Treat.*, **52**, 3445 (2014).
29. M. Fan, S. Tong and C. Q. Jia, *Int. J. Oil Gas Coal T.*, **8**, 489 (2014).
30. X. Zhang, W. Wang, S. Luo and Q. Lin, *J. Colloid Interface Sci.*, **553**, 484 (2019).
31. I. G. Stoycheva, B. G. Tsyntsarski, B. N. Petrova, B. Kumanek, T. K. Budinova and N. V. Petrov, *Water Air Soil Pollut.*, **227**, 452 (2016).
32. P. Yao, J. Cen, M. Fang, T. Wang and Q. Wang, *RSC Adv.*, **8**, 17558 (2018).
33. G. Asgari, B. Roshani and G. Ghanizadeh, *J. Hazard. Mater.*, **217-218**, 123 (2012).